Contribution of the *Scx*$^{+}$/*Sox9*$^{+}$ progenitor cell population to the establishment of the chondro-tendinous/ligamentous junction

Yuki Sugimoto[1], Aki Takimoto[1], Haruhiko Akiyama[2], Ralf Kist[3], Gerd Scherer[4], Takashi Nakamura[2], Yuji Hiraki[1], and Chisa Shukunami[1*]

[1]Department of Cellular Differentiation, Institute for Frontier Medical Sciences, Kyoto University, Kyoto 606-8507, Japan.

[2]Department of Orthopaedics, Faculty of Medicine, Kyoto University, Kyoto 606-8507, Japan.

[3]Centre for Oral Health Research, School of Dental Sciences, Newcastle University, Newcastle upon Tyne, United Kingdom.

[4]Institute of Human Genetics, Faculty of Medicine, University of Freiburg, Freiburg, Germany.

Running title: Role of Sox9 in the enthesis

Key words: Sox9; Scx; tenocytes; ligamentocytes; chondrocytes.

[*]Address correspondence to: Chisa Shukunami, D.D.S., PhD, 53 Shogoin-Kawahara-cho, Sakyo-ku, Kyoto, 606-8507, Japan.

Tel & Fax: +81-75-751-4633; E-mail: shukunam@frontier.kyoto-u.ac.jp

SUMMARY

Sox9 and *Scleraxis* (*Scx*) regulate cartilage and tendon formation, respectively. Here we report that *Scx*$^{+}$/*Sox9*$^{+}$ progenitors differentiate into chondrocytes and tenocytes/ligamentocytes to form the primordial enthesis, the junction between hyaline cartilage and tendon/ligament. *Sox9* lineage-tracing in the *Scx*$^{+}$ domain revealed that *Scx*$^{+}$ progenitors can be subdivided into two distinct populations with regard to their *Sox9* expression history, i.e. *Scx*$^{+}$/*Sox9*$^{+}$ and *Scx*$^{+}$/*Sox9*$^{-}$ progenitors. Tenocytes are derived from *Scx*$^{+}$/*Sox9*$^{+}$ and *Scx*$^{+}$/*Sox9*$^{-}$ progenitors. The closer the tendon is to the cartilaginous primordium, the more tenocytes arise from *Scx*$^{+}$/*Sox9*$^{+}$ progenitors. Ligamentocytes and annulus fibrosus cells of the intervertebral discs are descendants of *Scx*$^{+}$/*Sox9*$^{+}$ progenitors. Conditional inactivation of *Sox9* in *Scx*$^{+}$/*Sox9*$^{+}$ cells causes defective formation of the entheseal cartilages, tendons, ligaments, and the annulus fibrosus of the intervertebral discs. Thus, the *Scx*$^{+}$/*Sox9*$^{+}$ progenitor pool is a unique multipotent cell population that gives rise to tenocytes, ligamentocytes, and chondrocytes for the establishment of the chondro-tendinous/ligamentous junction.

INTRODUCTION

In vertebrates, the coordinated body movement is ensured by a close functional and physical association of bones, muscles, tendons, and ligaments. Tendons connect muscles to the skeletal components and function as the force transmitters, while ligaments bind bones together to stabilize joints (Benjamin and Ralphs, 2000; Rumian et al., 2007). Cells in tendons and ligaments are categorized as special types of fibroblasts known as tenocytes and ligamentocytes (Benjamin and Ralphs, 2000). Unlike randomly distributed fibroblasts in loose connective tissues, tenocytes and ligamentocytes in dense connective tissues are highly organized and align in rows between parallel thick fibers mainly consisting of type I collagen that provides the major resistance to tensile forces (Amiel et al., 1984; Canty et al., 2004). By inserting dense regular type I collagen fibers into muscle from the myotendinous junction and into bone from the osteo-tendinous/ligamentous junction called the enthesis, tendons and ligaments integrate each musculoskeletal component to establish a locomotive organ as one functional unit (Benjamin and Ralphs, 1998; Benjamin and Ralphs, 2000). To achieve this integration, progenitors for these cells need to be coordinately distributed at both sides of the junction and then execute each differentiation program there. However, it is still not clear how the coordinated assembly of the skeletal element and/or the muscle component through the tendon/ligament is established during development.

Progenitor cells for tendons, ligaments, cartilage, and bone arise from the sclerotome, the lateral plate mesoderm, and the neural crest (Akiyama et al., 2005; Christ et al., 2004; Mori-Akiyama et al., 2003; Smith et al., 2005), whereas myogenic

progenitors are derived from the myotome (Brent and Tabin, 2002). During the early stages of the musculoskeletal development, these progenitor populations migrate and settle down to the prospective region to give rise to cartilage, muscle, tendon, and ligament primordium (Kardon, 1998). Each primordium for the musculoskeletal component initially develops as an individual unit but later integrated with each other by a previously unknown mechanism.

Sox9, a SRY-related transcription factor containing a high-mobility-group box DNA-binding domain, is an important regulator for cartilage formation. In *Sox9*-deficient chimeric embryos generated by the injection of *Sox9*$^{-/-}$ embryonic stem (ES) cells into *Sox9*$^{+/+}$ blastocysts, *Sox9*$^{-/-}$ cells are eliminated from cartilaginous primordia and are instead incorporated into the surrounding connective tissues (Bi et al., 1999). Conditional inactivation studies of *Sox9* using *Prx1Cre* or *Col2a1Cre* mice have revealed that *Sox9* is required for multiple steps of chondrogenic differentiation before and after cartilaginous condensation (Akiyama et al., 2002). In the tendon and ligament cell lineage, *Scleraxis* (*Scx*), a basic helix-loop-helix transcription factor, is persistently expressed throughout differentiation (Pryce et al., 2007; Schweitzer et al., 2001). In *Scx*$^{-/-}$ mice, the intramuscular and force-transmitting tendons in the limbs and tail tendons become hypoplastic, although the short appendicular anchoring tendons and ligaments are not significantly affected (Murchison et al., 2007). Such differential dependence on *Scx* expression suggests that tendons consist of distinct cell populations that have not been defined yet.

At the early stages of the musculoskeletal development, both *Sox9* and *Scx* are detected in the subpopulation of tendon/ligament progenitors and chondroprogenitors

(Akiyama et al., 2005; Brent et al., 2005; Sugimoto et al., *in press*). *Sox9* is upregulated during chondrogenesis (Zhao et al., 1997), but its expression is downregulated in association with the formation of the cruciate ligaments of the knee joint, Achilles tendon, and patella tendon (Soeda et al., 2010). On the other hand, *Scx* expression in cartilaginous primordia is transient during chondrogenesis (Cserjesi et al., 1995; Sugimoto et al., *in press*). Lineage analysis using *ScxCre* Tg crossing with reporter mice revealed that *Scx* positive chondroprogenitors differentiate into chondrocytes around the chondro-tendinous/ligamentous junction (CT/LJ) during mouse development (Sugimoto et al. *in press*). These lines of evidence suggest that *Scx* and *Sox9* expression is coordinately regulated in the cell population bridging between cartilage and tendon/ligament. However, very little is known about the cellular origin or molecular mechanism to regulate the formation of the junction between cartilage and tendon/ligament.

Through the detailed *Sox9*-lineage tracing in Scx^+ cells, we found that the Scx^+ cell population can be divided into two distinct populations with or without their *Sox9* expression history, i.e. $Scx^+/Sox9^-$ and $Scx^+/Sox9^+$ progenitors. Tenocytes are derived from both $Scx^+/Sox9^-$ and $Scx^+/Sox9^+$ progenitors, while ligamentocytes arise from $Scx^+/Sox9^+$ progenitors. Chondrocytes around the CT/LJ are descendants of $Scx^+/Sox9^+$ progenitors. The closer the tendon is to the cartilaginous primordium, the more tenocytes arise from $Scx^+/Sox9^+$ progenitors. Using loss-of-function approaches, we demonstrate that $Scx^+/Sox9^+$ progenitors functionally contribute to the establishment of the junction between hyaline cartilage and tendon/ligament.

MATERIALS AND METHODS

Animals and embryos

Mice were purchased from Japan SLC, Inc. (Shizuoka, Japan) or from Shimizu Laboratory Supplies co. Ltd. (Kyoto, Japan). *ROSA26R* (*R26R*) (Soriano, 1999) or *Rosa-CAG-LSL-tdTomato* (*Ai14*) (Madisen et al., 2010) strains were crossed to generate the *Sox9$^{Cre/+}$;R26R* and *Sox9$^{Cre/+}$;Ai14* mice for *Sox9* lineage tracing. Ai14 mice harbor a targeted mutation of the *Gt(ROSA)26Sor* locus with a *loxP*-flanked STOP cassette preventing transcription of a CAG promoter-driven red fluorescent protein variant, tdTomato. Generation of *ScxGFP* and *ScxCre* transgenic strains has been previously reported (Sugimoto et al., *in press*). To generate *Sox9* conditional knock-out mice, *Sox9-flox* (Kist et al., 2002) and *ScxCre* transgenic strains were crossed. All of the animal experimental procedures used in this study were approved by the Animal Care Committee of the Institute for Frontier Medical Sciences, Kyoto University and conformed to institutional guidelines for the study of vertebrates.

In situ hybridization

The antisense RNA probes for each gene were transcribed from the linearized plasmids with a digoxygenin (DIG) RNA labeling kit (Roche) as previously described (Takimoto et al., 2009). For RNA probes, the cDNAs for *Scx* and *Myog* were amplified by RT-PCR based on its sequence information in GenBank (*Scx*, S78079; *Myog*, BC068019). Mouse *Sox9* cDNA was previously described (Wagner et al., 1994). For frozen section *in situ* hybridization, mouse embryos are treated in 20% sucrose without any fixation and then embedded in Tissue-Tek OCT compound (Sakura

Finetek). The embedded embryos were sliced at 8 μm thickness. Frozen sections were postfixed with 4% paraformaldehyde dissolved in phosphate-buffered saline (PFA/PBS) for 10 minutes at room temperature and then carbethoxylated twice in the 0.1% DEPC/PBS. Sections were treated in 5 x SSC, and hybridization was performed at 58˚C with DIG labeled antisense RNA probes. For whole mount *in situ* hybridization, mouse embryos were fixed with 4% PFA/PBS overnight. After fixation, embryos were gradually dehydrated with methanol. Prior to hybridization, embryos were rehydrated with PBS and treated with 2-5 μg/ml of proteinase K (Roche) at 25˚C. Hybridization was performed at 65˚C with DIG labeled antisense RNA probe for *Tnmd*. To detect DIG labeled RNA probes, immunological detection was performed with an anti-DIG antibody conjugated with alkaline phosphatase (Anti-DIG-AP Fab fragment; Roche) and BM purple (Roche).

Immunostaining

Embryos were fixed with 4% PFA/PBS at 4˚C for 3 hours, immersed in a series of sucrose solutions (12%, 15%, and 18% sucrose/PBS), frozen, and cryosectioned at a thickness of 8 μm. For *Sox9*$^{Cre/+}$*;R26R* mice, specimens were treated with 20% sucrose at 4˚C for 3 hours without prefixation, cryosectioned at a thickness of 10 μm, and then fixed with ice-cold acetone. After washing with PBST (phosphate-buffered saline containing 1% Tween 20), the slides were incubated with 2% skim milk in PBST for 20 min and incubated overnight at 4˚C with primary antibodies diluted with 2% skim milk in PBST. After washing, the sections were incubated with goat anti-rat and anti-rabbit secondary antibodies conjugated to Alexa Fluor 488 or with goat anti-rabbit

and anti-mouse secondary antibodies conjugated to Alexa Fluor 594, and washed again in PBST. The primary antibodies used were anti-GFP (diluted 1:1000; Nakarai), anti-Sox9 (diluted 1:600; Chemicon), anti-Tnmd (diluted 1:1000) (Oshima et al., 2004; Shukunami et al., 2008), anti-Chm1 (diluted 1:1000), and anti-type I collagen (diluted 1:500; Rockland), respectively. The purified ChM-I MoAb (clone: hCHM-05) is commercially available (Cosmo Bio Co., Ltd., Tokyo, Japan). Nuclei were counterstained with 4',6-Diamidino-2-phenylindole (DAPI). The images were captured under a Leica DMRXA microscope equipped with a Leica DC500 camera (Leica Microsystems, Wetzlar).

Toluidine blue and X-gal staining

For toluidine blue staining, deparaffinized and/or hydrated sections were stained with a 0.05% toluidine blue solution (pH 4) for 2 to 5 min as previously described (Takimoto et al., 2012). For X-gal staining, embryos were treated with 20% sucrose/PBS at 4˚C, and embedded in Tissue-Tek OCT compound (Sakura Finetek). Frozen sections were prepared at a thickness of 14 μm. Before staining, the sections were treated with fixation solution (0.2% glutaraldehyde, 5 mM EGTA, and 2 mM $MgCl_2$) at 4˚C for 5 min. After washing (phosphate buffer containing 2 mM $MgCl_2$, 0,01% sodium deoxycholate, and 0.02% Nonidet P-40), the sections were incubated with X-gal staining solution (5 mM potassium ferrocyanide, 5 mM potassium ferricyanide, and 1 mg/ml X-gal) at 37˚C overnight.

Skeletal preparations

After fixation with 4% PFA/PBS, mouse embryos were dehydrated with ethanol. Skin and soft tissues were removed, and the embryos were then stained with 0.015% Alcian blue 8GX (Sigma). After clearing with 2% KOH, the embryos were stained with 0.05% alizarin red in 1% KOH and then cleared with 1% KOH.

RESULTS

The Scx^+ cell population in the axial and the appendicular mesenchyme contains two distinct subpopulations: $Scx^+/Sox9^+$ and $Scx^+/Sox9^-$ progenitors.

Scx is expressed in the tendogenic/ligamentogenic regions as well as the chondrogenic regions (Cserjesi et al., 1995; Sugimoto et al., *in press*). *In situ* hybridization analysis revealed that *$Scx^+/Sox9^+$* chondrogenic cells are predominantly distributed in and around the primordial enthesis between cartilage and tendon/ligament (Fig. S1). To compare the expression domains of Sox9 in Scx^+ cells in more detail, we established a transgenic mouse line expressing *enhanced green fluorescent protein* (*EGFP*) under the control of promoter and enhancers of mouse *Scx* (*ScxGFP*) (Sugimoto et al., *in press*) and performed double immunostaining using antibodies against Sox9 and GFP in transgenic *ScxGFP* embryos (Fig. 1).

During axial musculoskeletal development, the paraxial mesoderm separates into the somites that eventually give rise to the vertebrae, ribs, tendons, ligaments, the dermis of the dorsal skin, and muscles (Christ et al., 2004; Christ et al., 2000). In the thoracic somite at E10.5, Sox9 was expressed in the entire sclerotome, notochord, and neural tube (Fig. 1A), while the dorsolateral sclerotome containing tendon

progenitors was composed of Scx^+ cells (Fig. 1B). The dorsolateral sclerotome was positive for Sox9, but a small number of $Scx^+/Sox9^+$ and $Scx^+/Sox9^-$ cells were observed in the dermomyotome (Fig. 1C). At E11.5, $Scx^+/Sox9^+$ cells were observed in the vertebral and rib primordia (Fig. S2A,B), and $Scx^-/Sox9^+$ cells were surrounded by $Scx^+/Sox9^+$ and $Scx^+/Sox9^-$ cells (Fig. S2C). At E13.5, Sox9 was detected in the cartilaginous primordia of the vertebral body, neural arch, and ribs (Fig. 1D). In contrast, Scx was exclusively expressed in the vertebral and costal tendon primordia (Fig. 1E). As typically seen in the costal region, Sox9 and Scx exhibited non-overlapping expression patterns at this stage (Fig. 1F).

Appendicular and abdominal muscles are derived from the hypaxial myotome, whereas lateral plate mesoderm gives rise to the skeletal elements, tendons, and ligaments of limbs (Brent and Tabin, 2002). At E10.5, the overlapping expression of Sox9 and Scx was observed in the limb bud mesenchyme except for the distal region (Fig. 1G-I). In the forelimb at E11.5, the primordia of the radius, ulna, carpal, and metacarpal bone express *Sox9.* $Scx^+/Sox9^+$ or $Scx^+/Sox9^-$ cells then rearrange into the dorsal and ventral superficial regions surrounding the $Sox9^+$ region (Fig. S2D-F). The $Scx^+/Sox9^+$ region was observed at the most proximal region (Fig. S2F). At E13.5, the appendicular cartilaginous elements were single positive for Sox9 (Fig. 1J), but the collateral ligaments and the interzone of the metacarpophalangeal joint were double-positive for Sox9 and Scx (Fig. 1K). At E14.5, $Scx^+/Sox9^+$ and $Scx^+/Sox9^-$ cells were present in the cartilage of the nasal septum and the fibrous cells of the turbinate primordia, respectively (Fig. 1L). In the vertebral column, the outer layer of the intervertebral discs was shown to be Scx^+ (Fig. 1M). $Scx^+/Sox9^+$ chondrogenic cells

were found in the entheseal region of the Achilles tendon and the patella (Fig. 1N,O).

Based on these data, we conclude that the Scx^+ cell population can be subdivided into two distinct subpopulations: $Scx^+/Sox9^+$ and $Scx^+/Sox9^-$ progenitors, and that *Sox9* expression later disappeared in tendons and ligaments as differentiation process proceeds.

The *Scx*$^+$*/Sox9*$^+$ progenitor pool is a unique multipotent cell population that gives rise to chondrocytes, tenocytes, and ligamentocytes.

For lineage-tracing of *Sox9*$^+$ cells in the Scx^+ domains during tendon and ligament formation, we crossed *Sox9*$^{Cre/+}$ mice (Akiyama et al., 2005) with the Cre reporter line *Rosa-CAG-LSL-tdTomato* (*Ai14*) (Madisen et al., 2010) to generate *Sox9*$^{Cre/+}$*;Ai14* mice, which were then crossed with *ScxGFP* mice to obtain *Sox9*$^{Cre/+}$*;Ai14;ScxGFP* embryos (Fig. 2A-E, Fig. 3A-G).

In *Sox9*$^{Cre/+}$*;Ai14;ScxGFP* embryos at E14.5, cells with the *Sox9*$^+$ cell lineage were found in the tendons near the vertebral columns, ribs, joints between the ribs and vertebrae, and the developing lung (Fig. 2A). The outer fibrous region of the vertebrae and surrounding membranous regions consisted of *Scx*$^+$ cells with their *Sox9* expression history (Fig. 2B). In the tendinous diaphragm near the heart, most cells were negative for *Sox9* and single-positive for *Scx* (Fig. 2C). Abdominal tendons were single positive for *Scx* (Fig. 2D). In the tail, the insertion sites of the tendons into the vertebrae were derived from *Scx*$^+$*/Sox9*$^+$ progenitors, whilst tendons located further away from vertebrae were almost exclusively *Sox9*-negative and *Scx* single-positive (Fig. 2E).

We then analyzed the contribution of *Sox9*$^{+}$ progenitors in the lumbar vertebrae and their associated tendons/ligaments of *Sox9*$^{Cre/+}$*;Ai14* neonates at the level of the vertebral body, the articular process, or the spinous process (Fig. 2F-H, supplementary material Table S1). At P0, tendons and ligaments in the vicinity of vertebrae were derived from the *Sox9*$^{+}$ progenitor population (Fig. 2F-H). The lateral region of the thoracolumbar fascia enclosing the erector spinae muscles and tendons anchoring the latissimus dorsi muscle were negative for *Sox9* at P0 (Fig. 2H, T4, T3). Thus, *Scx*$^{+}$*/Sox9*$^{+}$ progenitors contribute to the formation of ligaments and tendons in the vicinity of ribs and vertebrae, while abdominal tendons are derived from the *Scx*$^{+}$*/Sox9*$^{-}$ cell lineage.

In the distal part of the hindlimb of *Sox9*$^{Cre/+}$*;Ai14;ScxGFP* embryos at E14.5, the ligaments arose from *Scx*$^{+}$*/Sox9*$^{+}$ progenitors, but both *Scx*$^{+}$*/Sox9*$^{+}$ and *Scx*$^{+}$*/Sox9*$^{-}$ progenitors contributed to tendon formation (Fig. 3A). *Scx*$^{+}$*/Sox9*$^{+}$ progenitors contributed to the formation of collateral ligaments (Fig. 3B, L3) and tendons near the entheses (Fig. 3C,D), whereas other parts of tendons mainly arose from *Scx*$^{+}$*/Sox9*$^{-}$ progenitors and the proportion of these cells varied between the individual tendons. For instance, extensor digitorum longus tendon was derived from *Scx*$^{+}$*/Sox9*$^{-}$ progenitors except for the prospective enthesis (Fig. 3B, T8), while Achilles tendons arose from both the *Scx*$^{+}$*/Sox9*$^{+}$ and *Scx*$^{+}$*/Sox9*$^{-}$ cell lineage (Fig. 3C-D, T9).

In the knee joint at E14.5, the primordia for cruciate and patella ligaments were visible as the *Scx*$^{+}$ region within the prospective joint cavity (Fig. 3E). All of the articular components and cartilage were positive for *Sox9* (Fig. 3F). The developing cruciate ligaments and capsular ligaments including the patella ligament and tibial

collateral ligament were *Sox9*-positive (Fig. 3G). In cruciate and patella ligaments at P0, Sox9 protein was no longer detected in these tendons or ligaments except for cartilage (Fig. 3H,I). Thus, all appendicular ligamentocytes arise from *Scx*$^{+}$/*Sox9*$^{+}$ progenitors, whereas appendicular tenocytes are derived from both the *Scx*$^{+}$/*Sox9*$^{+}$ and the *Scx*$^{+}$/*Sox9*$^{-}$ cell lineage. Taken together with these findings, the *Scx*$^{+}$/*Sox9*$^{+}$ progenitor pool is a unique multipotent cell population that gives rise to *Scx*$^{-}$/*Sox9*$^{+}$ chondrocytes and *Scx*$^{+}$/*Sox9*$^{-}$ tenocytes/ligamentocytes.

The closer the tendon is to the cartilaginous primordium, the more tenocytes arise from the *Sox9*$^{+}$ cell lineage.

To investigate how *Sox9*$^{+}$ progenitors contribute to limb tendon formation, we analyzed the distribution of cells with the *Sox9*$^{+}$ cell lineage in Tnmd-positive mature tendons and Chondromodulin-1 (Chm1)-positive mature cartilage in the forearm of the *Sox9*$^{Cre/+}$*;R26R* mice at P0 (Fig. 4A-L, supplementary material Table S1). Chm1 and Tnmd are markers of mature chondrocytes and tenocytes/ligamentocytes, respectively (Oshima et al., 2004; Shukunami et al., 2008; Shukunami et al., 2006).

Within the proximal parts of the ulna and radius, the sheet-like anchoring tendons consisted of tenocytes derived from *Sox9*$^{+}$ progenitors (Fig. 4A,G). In contrast, at the medial side of the ulna and radius, *Sox9*$^{+}$ progeny was not present in the proximal region of the cord-like force-transmitting tendons that were inserted into the individual muscles (Fig. 4B,H). However, tenocytes derived from *Sox9*$^{+}$ progenitors were found in the bundled force-transmitting tendons in the dorsal region of the distal ulna and radius and of the carpal levels (Fig. 4C,D,I,J). The forearm at the wrist level can be

subdivided into several extensor tendon compartments with thick fascia. Within the same compartment, each tendon was derived from *Sox9*$^{+}$ and *Sox9*$^{-}$ progenitors, and the ratio of *Sox9*$^{+}$ to *Sox9*$^{-}$ progenitor-derived tenocytes was similar (Fig. 4I,J). In carpal tendons, more tenocytes derived from *Sox9*$^{+}$ progenitors were observed (Fig. 4D,J). Tendons containing many *Sox9*$^{+}$ cells were inserted into the proximal edges of the metacarpals or carpals, whereas tendons containing less or no *Sox9*$^{+}$ cells were inserted into the middle or distal phalanges, in the more distal region of the autopod (Fig. 4D,J).

Around the metacarpal level, bundled tendons separate into individual tendons that insert into the end point of each digit (Fig. 4E,F). More tenocytes of the *Sox9*$^{+}$ cell lineage were observed in the tendons at the palmar side including tendons of the flexor digitorum profundus (T26), flexor digitorum sublimis (T27), and interosseous (T30) (Fig. 4K,L), whilst most dorsal tendons (T18, T19) were negative for *Sox9* (Fig. 4E,K). In the collateral ligaments (L9) of the metacarpophalangeal joint, all ligamentocytes were strongly positive for *Sox9* (Fig. 4F,L). Although the force transmitting tendons were derived from both *Sox9*$^{+}$ and *Sox9*$^{-}$ progenitors, the anchoring tendons near the elbow wholly arose from *Sox9*$^{+}$ progenitors (Fig. 4M). Taken together, the proportion of tenocytes with their *Sox9*$^{+}$ expression history varies between the individual force-transmitting tendons but generally, the number of these *Sox9*$^{+}$ tenocytes decreases with increasing distance from the skeletal element.

Characterization of the transitional zone between cartilage and tendon/ligament.

We then focused our analysis on the transitional zone between cartilage and tendon/ligament, to reveal the contribution of Sox9^{+} progenitors to the entheses. Entheses are classified into two groups: fibrous and fibrocartilaginous entheses (Benjamin and Ralphs, 2001). Collagen fibers in the fibrous entheses are inserted into bone via the periosteum which gives firmer hold to the tendons and ligament, while the fibrocartilaginous entheses have four zones during the transition from tendon/ligament to bone, consisting of tendon/ligament, fibrocartilage, mineralized fibrocartilage, and bone. Fibrous entheses are mainly present in short ligament or tendons. Since periosteum has been reported to be derived from Sox9^{+} progenitors (Akiyama et al., 2005), we examined the prospective fibrocartilaginous entheses of quadriceps femoris tendon, cruciate ligaments, and the Achilles tendon in *Sox9$^{Cre/+}$;R26R* mice (Fig. 5). Type I collagen (Col1) and Chm1 were localized to tendons/ligaments including the prospective entheseal region and hyaline cartilage, respectively (Fig. 5A,D,G), whilst Tnmd was expressed in tendons and ligaments except for the region just adjacent to hyaline cartilage (Fig. 5B,E,H). These Col1+/Tnmd- cells were X-gal positive (Fig. 5C,F,I). Hence, near the joint region, tenocytes, ligamentocytes, and chondrocytes were derived from Sox9+ progenitors, but the prospective entheseal region abutting hyaline cartilage was negative for both Tnmd and Chm1, suggesting the presence of a distinct population in the prospective fibrocartilaginous enthesis bridging between tendons/ligaments and hyaline cartilage.

Skeletal defects by conditional inactivation of *Sox9* in *Scx^{+}/Sox9^{+}* cells.

We have previously reported generation of two lines of transgenic mouse lines that

express *Cre recombinase* in the *Scx*$^{+}$ domains at high (*ScxCre-H*) or low (*ScxCre-L*) levels (Sugimoto et al., *in press*). Due to the expression gradient and transient expression of *Scx* around the entheseal cartilage (Fig. S1), more chondrocytes in *ScxCre-H* are *Scx*$^{+}$ than those in *ScxCre-L* (Sugimoto et al., *in press*). To investigate the functional role of *Sox9* in *Scx*$^{+}$/*Sox9*$^{+}$ cells by a loss of function approach, we crossed these lines with *Sox9-flox* mice to inactivate *Sox9* in *Scx*$^{+}$ cells (Kist et al., 2002). Both *ScxCre-L;Sox9*$^{flox/+}$ and *ScxCre-H;Sox9*$^{flox/+}$mice were viable and fertile, but *ScxCre-L;Sox9*$^{flox/flox}$ and *ScxCre-H;Sox9*$^{flox/flox}$ mice died after birth. In *ScxCre-H;Sox9*$^{flox/flox}$ mice, severe skeletal hypoplasia were observed beyond the prospective entheseal cartilage, thus causing the secondary defects in tenocytes derived from *Scx*$^{+}$/*Sox9*$^{-}$ cells (not shown). Thus, we analyzed *ScxCre-L;Sox9*$^{flox/flox}$ mice with the skeletal defects around the entheseal cartilage in more detail.

In *ScxCre-L;Sox9*$^{flox/flox}$ neonates, sternum and the ribcage except for the proximal region are missing (Fig. 6A-D). In the vertebral column of *ScxCre-L;Sox9*$^{flox/flox}$ at E18.5, the vertebral bodies, the intervertebral discs, the articular processes of the neural arch, the transverse processes were hypoplastic (Fig. 6E,F). Severe hypoplasia in the ribcage is expected from the expression of *Scx* in the early stages of costal cartilage formation (Fig. 6M-O). The appendages of *ScxCre-L;Sox9*$^{flox/flox}$ are shorter and hypoplastic than that of control and the joint cavity was smaller (Fig. 6A,B, G-L). In the forelimb of *ScxCre-L;Sox9*$^{flox/flox}$, hypoplasia of carpal bones at the ulnar side, elbow joint, cartilage around the shoulder joint, deltoid tuberosity of the humerus was evident and the curvature of the wrist was observed (Fig. 6G,H). Interestingly, abnormal mineralization occurred in the olecranon (Fig. 6G,H). In the hindlimb of

ScxCre-L;Sox9$^{flox/flox}$, tarsal bones, cartilage around the hip and the knee joint, and tibial tuberosity were defective (Fig. 6I,J) and the patella within the patella ligament was missing (Fig. 6K,L). Thus, these results suggest that skeletal dysplasia is observed in the Scx^{+} cartilaginous region that is closely associated with tendons and ligaments.

Defective formation of the junction bridging between cartilage and tendon/ligament by conditional inactivation of *Sox9* in *Scx*$^{+}$*/Sox9*$^{+}$ cells.

Double immunostaining of Tnmd and Chm1 revealed defective formation of the junction between cartilage and tendon/ligament in *ScxCre-L;Sox9*$^{flox/flox}$ at E18.5. Transverse process of the lumber vertebrae (Fig. 7C) and the lateral region of sacral vertebrae (Fig. 7A) provide the attachment sites for axial tendons, but these sites are missing in *ScxCre-L;Sox9*$^{flox/flox}$ (Fig. 7B,D). In control mice, Sox9^{+} cells are scattered in the outer annulus fibrosus near the inner annulus fibrosus (Fig. 7E), while these cells are missing in *ScxCre-L;Sox9*$^{flox/flox}$ (Fig. 7F). In the intervertebral discs of *ScxCre-L;Sox9*$^{flox/flox}$, formation of the inner annulus fibrosus showing metachromatic staining with toluidine blue was defective, but the outer annulus fibrosus became wider (Fig. 7H), compared to control mice (Fig. 7G). Thus, in *ScxCre-L;Sox9*$^{flox/flox}$, the prospective entheses were either missing or hypoplastic in the axial skeleton.

In the appendicular skeleton, hypoplastic tendon formation in association with severe defects in skeletal formation at the ulnar side (Fig. 6G,H) was observed in *ScxCre-L;Sox9*$^{flox/flox}$ at E18.5 (not shown). In the knee joint, patella and the frontal region of the femoral condyle are missing (Fig. 7I,J). In the heel, the attachment site

for the Achilles tendon was defective (Fig. 7K-N). Interestingly, cells just adjacent to the tendon attachment site are positive for *Sox9* in control mice, whereas such Sox9^{+} cells were missing in *ScxCre-L;Sox9*$^{flox/flox}$ (Fig. 7O,P).

DISCUSSION

In our current study, we have demonstrated for the first time that the *Scx*$^{+}$ cell population can be subdivided into two distinct populations with regard to their *Sox9* expression history, i.e. *Scx*$^{+}$/*Sox9*$^{+}$ and *Scx*$^{+}$/*Sox9*$^{-}$ progenitors. The *Scx*$^{+}$/*Sox9*$^{+}$ progenitor pool is a unique multipotent cell population that gives rise to *Scx*$^{-}$/*Sox9*$^{+}$ chondrocytes and *Scx*$^{+}$/*Sox9*$^{-}$ tenocytes/ligamentocytes (Fig. 8A). The closer the tendon and cartilage are to the prospective enthesis, the more tenocytes and chondrocytes originate from *Scx*$^{+}$/*Sox9*$^{+}$ progenitors (Fig. 8B). Further analyses of *ScxCre;Sox9*$^{flox/flox}$ mice revealed that the *Scx*$^{+}$/*Sox9*$^{+}$ cell population functionally contribute to the establishment of the junction between cartilage and tendon/ligament.

The *Scx*$^{+}$/*Sox9*$^{+}$ progenitor pool is a multipotent cell population that gives rise to tenocytes, ligamentocytes, annulus fibrosus cells of intervertebral discs, and chondrocytes.

Tenocytes are descendants of *Scx*$^{+}$/*Sox9*$^{+}$ and *Scx*$^{+}$/*Sox9*$^{-}$ progenitors (Fig. 8A). In general, the number of tenocytes with their *Sox9* expression history decreases with increasing distance from the skeletal element. Ligamentocytes and annulus fibrosus cells in intervertebral discs are derived from *Scx*$^{+}$/*Sox9*$^{+}$ progenitors, whereas chondrocytes are derived from *Scx*$^{+}$/*Sox9*$^{+}$ and *Scx*$^{-}$/*Sox9*$^{+}$ progenitors (Fig. 8A). The

closer the cartilage is to the prospective entheses, the more chondrocytes arise from *Scx*$^{+}$/*Sox9*$^{+}$ progenitors. Thus, the *Scx*$^{+}$/*Sox9*$^{+}$ progenitor cell population is predominantly distributed across the enthesis to form the chondro-tendinous/ligamentous junction during development (Fig. 8B).

In contrast to the axial tendon formation, very little is known about the axial ligament formation. We show that the *Scx*$^{+}$ axial ligaments are derived from the *Sox9*$^{+}$ cell lineage. Since axial ligamentocytes are derived from the *Sox9*$^{+}$ cell lineage, we conclude that these *Scx*$^{+}$ ligamentocytes originate from the *Sox9*$^{+}$ sclerotome. However, the timing of *Scx* expression in *Sox9*$^{+}$ ligament progenitors needs to be further investigated to clarify whether the axial ligament progenitors are derived from the *Scx*$^{+}$/*Sox9*$^{+}$ dorsolateral domain of the sclerotome or are recruited from the *Scx*$^{-}$ sclerotome to express *Scx* at later stages of development.

The appendicular tendons include a considerable number of tenocytes derived from *Scx*$^{+}$/*Sox9*$^{-}$ progenitors, particularly in the distal part of the limbs. Unlike the sclerotome consisting of *Sox9*$^{+}$ progenitors, both *Sox9*$^{+}$ and *Sox9*$^{-}$ progenitors are present in the lateral plate mesoderm of limb bud at E10.5. The *Scx*$^{+}$/*Sox9*$^{-}$ population in the lateral plate mesoderm may represent the prospective distal tendon progenitors, although we cannot exclude the possibility that another as-yet-unknown populations of tendon progenitors are recruited from the surrounding tissue to become *Scx*$^{+}$ tenocytes later in development.

Scx^{+}*/Sox9*$^{+}$ progenitor cells contribute to the establishment of the CT/LJ.

In *ScxCre;Sox9*$^{flox/flox}$ mice, the attachment sites of tendons/ligaments into

cartilaginous primordia and annulus fibrosus of intervertebral discs between vertebrae are severely impaired. The most notable phenotype of *ScxCre;Sox9*$^{flox/flox}$ embryos is an absence of the ribcage. Chondrogenic cells in the developing costal cartilage have the ability to differentiate into entheseal chondrocytes as evidenced by the expression of *Scx* in the entire rib cartilaginous primordium. This is compatible with the histological feature that costal chondrocytes are located very close to the tendinous attachment site of the surrounding intercostal muscle to each rib cartilage. Likewise, patella cartilage embedded in the tendon and cartilaginous long bone primordia such as ulna and fibula with their attachment site of the interosseus membrane and anchoring tendons are missing. Thus, our loss of function analysis of *Sox9* in the *Scx*$^{+}$ domain revealed the functional significance of the *Scx*$^{+}$/*Sox9*$^{+}$ progenitor cell population in the establishment of the chondro-tendinous/ligamentous junction, especially in the cartilaginous side.

In *Sox9*$^{flox/flox}$*;Prx1-Cre* mice, inactivation of *Sox9* in limb bud mesenchyme causes complete absence of cartilage and bone (Akiyama et al., 2002). Severe chondrodysplasia also occurs in *Sox9*$^{flox/flox}$*;Col2a1-Cre* by inactivation of *Sox9* in precartilaginous condensing cells and chondrocytes (Akiyama et al., 2002). Based on these findings, functional roles of *Sox9* in chondrogenesis could be discussed at three critical stages: chondroprogenitor stage, cartilaginous condensation stage, and chondrocyte stage. Similarly, we propose to discuss tendo/ligamentogenesis in three distinct stages: tendon/ligament progenitor stage, tendon/ligament primordium formation stage, and tenocyte/ligamentocyte stage. In *ScxCre;Sox9*$^{flox/flox}$, we observed severe hypoplasia of the entheses of tendons/ligaments, annulus fibrosus of

intervertebral discs, and cartilages arising from *Scx*$^{+}$*/Sox9*$^{+}$ chondroprogenitors. The longer *Sox9* expression continues, the severer the defects within the *Scx*$^{+}$*/Sox9*$^{+}$ domain of *ScxCre;Sox9*$^{flox/flox}$ embryos become. Unlike chondrogenic cells, which continuously express *Sox9*, *Sox9* was downregulated in the migrating tendon/ligament progenitors before their arrival at the presumptive tendon- or ligamento-forming site. Considering the timing of *Sox9* downregulation in the tendon/ligament cell lineages, it is unlikely that the last two stages during tendo/ligamentogenesis critically depend on the function of *Sox9*. Loss of *Sox9* in *Scx*$^{+}$*/Sox9*$^{+}$ progenitors is likely a main cause of the hypoplastic chondro-tendinous/ligamentous junction in *ScxCre;Sox9*$^{flox/flox}$.

Intervertebral discs and joints connect adjacent vertebrae. Each intervertebral disc is composed of an external annulus fibrosus surrounding the internal nucleus pulposus. Cells in the annulus fibrosus of intervtertebral discs can be traced back to somitocoele cells included in the central core of the somite, distinct from the progenitor population for the vertebral body (Mittapalli et al., 2005). The annulus fibrosus consists of the inner annulus with chondrocytic cells and the outer annulus with tenocytic cells. We have shown here that both types of cells arise from *Scx*$^{+}$*/Sox9*$^{+}$ progenitors. In *ScxCre;Sox9*$^{flox/flox}$ mice, the inner annulus is missing but expansion of the outer annulus takes place on the ventral side. Thus, it is suggested that *Sox9* maintains the proper balance between the inner and the outer cell numbers by regulating survival and differentiation of cells in the inner annulus during intervertebral disc formation.

During postnatal growth, entheseal fibrocartilage develops in response to

compressive loads (Benjamin and Ralphs, 1998). Fibrocartilage is an important connective structure between tendon and hyaline cartilage, but its cellular origin remains uncertain. We show that Tnmd and Chm1 are expressed in tendon/ligament and hyaline cartilage, respectively, whereas the transitional region just adjacent to hyaline cartilage or tendon/ligament was negative for Tnmd and Chm1, consistent with our previous observation in rabbits (Yukata et al., 2010). Our lineage analysis further revealed that cells in this Tnmd$^-$/Chm1$^-$ zone are positive for *Sox9* and *Scx*. Therefore, it is likely that cells in this transitional zone give rise to fibrochondrocytes during the postnatal development. Further studies to reveal the cellular origin of fibrochondrocytes are now underway by using *Sox9CreERT2* and *ScxCreERT2* mice.

Acknowledgements

We thank Mr. T. Matsushita and Ms. K. Kogishi for the histological studies and Ms. H. Sugiyama for her valuable secretarial help. This study was partly supported by Grants-in-Aid from the Ministry of Education, Culture, Sport, Science and Technology of Japan.

The abbreviation used are: *Scx*, *Scleraxis*; *Sox9*, *Sry-box containing gene 9*; Tnmd, Tenomodulin; Chm1, Chondromodulin1; *Myog*, *Myogenin*.

References

Akiyama, H., Chaboissier, M. C., Martin, J. F., Schedl, A. and de Crombrugghe, B. (2002). The transcription factor Sox9 has essential roles in successive steps of the

chondrocyte differentiation pathway and is required for expression of Sox5 and Sox6. *Genes Dev* **16**, 2813-28.

Akiyama, H., Kim, J. E., Nakashima, K., Balmes, G., Iwai, N., Deng, J. M., Zhang, Z., Martin, J. F., Behringer, R. R., Nakamura, T. et al. (2005). Osteo-chondroprogenitor cells are derived from Sox9 expressing precursors. *Proc Natl Acad Sci U S A* **102**, 14665-70.

Amiel, D., Frank, C., Harwood, F., Fronek, J. and Akeson, W. (1984). Tendons and ligaments: a morphological and biochemical comparison. *J Orthop Res* **1**, 257-65.

Benjamin, M. and Ralphs, J. R. (1998). Fibrocartilage in tendons and ligaments--an adaptation to compressive load. *J Anat* **193 (Pt 4)**, 481-94.

Benjamin, M. and Ralphs, J. R. (2000). The cell and developmental biology of tendons and ligaments. *Int Rev Cytol* **196**, 85-130.

Benjamin, M. and Ralphs, J. R. (2001). Entheses--the bony attachments of tendons and ligaments. *Ital J Anat Embryol* **106**, 151-7.

Bi, W., Deng, J. M., Zhang, Z., Behringer, R. R. and de Crombrugghe, B. (1999). Sox9 is required for cartilage formation. *Nat Genet* **22**, 85-9.

Brent, A. E., Braun, T. and Tabin, C. J. (2005). Genetic analysis of interactions between the somitic muscle, cartilage and tendon cell lineages during mouse development. *Development* **132**, 515-28.

Brent, A. E. and Tabin, C. J. (2002). Developmental regulation of somite derivatives: muscle, cartilage and tendon. *Curr Opin Genet Dev* **12**, 548-57.

Canty, E. G., Lu, Y., Meadows, R. S., Shaw, M. K., Holmes, D. F. and Kadler, K. E. (2004). Coalignment of plasma membrane channels and protrusions (fibripositors)

specifies the parallelism of tendon. *J Cell Biol* **165**, 553-63.

Christ, B., Huang, R. and Scaal, M. (2004). Formation and differentiation of the avian sclerotome. *Anat Embryol (Berl)* **208**, 333-50.

Christ, B., Huang, R. and Wilting, J. (2000). The development of the avian vertebral column. *Anat Embryol (Berl)* **202**, 179-94.

Cserjesi, P., Brown, D., Ligon, K. L., Lyons, G. E., Copeland, N. G., Gilbert, D. J., Jenkins, N. A. and Olson, E. N. (1995). Scleraxis: a basic helix-loop-helix protein that prefigures skeletal formation during mouse embryogenesis. *Development* **121**, 1099-110.

Kardon, G. (1998). Muscle and tendon morphogenesis in the avian hind limb. *Development* **125**, 4019-32.

Kist, R., Schrewe, H., Balling, R. and Scherer, G. (2002). Conditional inactivation of Sox9: a mouse model for campomelic dysplasia. *Genesis* **32**, 121-3.

Madisen, L., Zwingman, T. A., Sunkin, S. M., Oh, S. W., Zariwala, H. A., Gu, H., Ng, L. L., Palmiter, R. D., Hawrylycz, M. J., Jones, A. R. et al. (2010). A robust and high-throughput Cre reporting and characterization system for the whole mouse brain. *Nat Neurosci* **13**, 133-40.

Mittapalli, V. R., Huang, R., Patel, K., Christ, B. and Scaal, M. (2005). Arthrotome: a specific joint forming compartment in the avian somite. *Dev Dyn* **234**, 48-53.

Mori-Akiyama, Y., Akiyama, H., Rowitch, D. H. and de Crombrugghe, B. (2003). Sox9 is required for determination of the chondrogenic cell lineage in the cranial neural crest. *Proc Natl Acad Sci U S A* **100**, 9360-5.

Murchison, N. D., Price, B. A., Conner, D. A., Keene, D. R., Olson, E. N., Tabin, C.

J. and Schweitzer, R. (2007). Regulation of tendon differentiation by scleraxis distinguishes force-transmitting tendons from muscle-anchoring tendons. *Development* **134**, 2697-708.

Oshima, Y., Sato, K., Tashiro, F., Miyazaki, J., Nishida, K., Hiraki, Y., Tano, Y. and Shukunami, C. (2004). Anti-angiogenic action of the C-terminal domain of tenomodulin that shares homology with chondromodulin-I. *J Cell Sci* **117**, 2731-44.

Pryce, B. A., Brent, A. E., Murchison, N. D., Tabin, C. J. and Schweitzer, R. (2007). Generation of transgenic tendon reporters, ScxGFP and ScxAP, using regulatory elements of the scleraxis gene. *Dev Dyn* **236**, 1677-82.

Rumian, A. P., Wallace, A. L. and Birch, H. L. (2007). Tendons and ligaments are anatomically distinct but overlap in molecular and morphological features--a comparative study in an ovine model. *J Orthop Res* **25**, 458-64.

Schweitzer, R., Chyung, J. H., Murtaugh, L. C., Brent, A. E., Rosen, V., Olson, E. N., Lassar, A. and Tabin, C. J. (2001). Analysis of the tendon cell fate using Scleraxis, a specific marker for tendons and ligaments. *Development* **128**, 3855-66.

Shukunami, C., Takimoto, A., Miura, S., Nishizaki, Y. and Hiraki, Y. (2008). Chondromodulin-I and tenomodulin are differentially expressed in the avascular mesenchyme during mouse and chick development. *Cell Tissue Res* **332**, 111-22.

Shukunami, C., Takimoto, A., Oro, M. and Hiraki, Y. (2006). Scleraxis positively regulates the expression of tenomodulin, a differentiation marker of tenocytes. *Dev Biol* **298**, 234-47.

Smith, T. G., Sweetman, D., Patterson, M., Keyse, S. M. and Munsterberg, A. (2005). Feedback interactions between MKP3 and ERK MAP kinase control scleraxis

expression and the specification of rib progenitors in the developing chick somite. *Development* **132**, 1305-14.

Soeda, T., Deng, J. M., de Crombrugghe, B., Behringer, R. R., Nakamura, T. and Akiyama, H. (2010). Sox9-expressing precursors are the cellular origin of the cruciate ligament of the knee joint and the limb tendons. *Genesis* **48**, 635-44.

Soriano, P. (1999). Generalized lacZ expression with the ROSA26 Cre reporter strain. *Nat Genet* **21**, 70-1.

Sugimoto, Y., Takimoto, A., Hiraki, Y. and Shukunami, C. Generation and characterization of ScxCre transgenic mice. *Genesis*. doi: 10.1002/dvg.22372.

Takimoto, A., Nishizaki, Y., Hiraki, Y. and Shukunami, C. (2009). Differential actions of VEGF-A isoforms on perichondrial angiogenesis during endochondral bone formation. *Dev Biol* **332**, 196-211.

Takimoto, A., Oro, M., Hiraki, Y. and Shukunami, C. (2012). Direct conversion of tenocytes into chondrocytes by Sox9. *Exp Cell Res* **318**, 1492-507.

Wagner, T., Wirth, J., Meyer, J., Zabel, B., Held, M., Zimmer, J., Pasantes, J., Bricarelli, F. D., Keutel, J., Hustert, E. et al. (1994). Autosomal sex reversal and campomelic dysplasia are caused by mutations in and around the SRY-related gene SOX9. *Cell* **79**, 1111-20.

Yukata, K., Matsui, Y., Shukunami, C., Takimoto, A., Hirohashi, N., Ohtani, O., Kimura, T., Hiraki, Y. and Yasui, N. (2010). Differential expression of Tenomodulin and Chondromodulin-1 at the insertion site of the tendon reflects a phenotypic transition of the resident cells. *Tissue Cell* **42**, 116-20.

Zhao, Q., Eberspaecher, H., Lefebvre, V. and De Crombrugghe, B. (1997).

Parallel expression of Sox9 and Col2a1 in cells undergoing chondrogenesis. *Dev Dyn* **209**, 377-86.

FIGURE LEGENDS

Fig. 1. Distribution of Sox9$^+$ and Sox9$^-$ cells in the Scx$^+$ region of mouse embryos.

(**A-O**) In *ScxGFP* transgenic mouse embryos, Sox9$^+$ (red) and Scx$^+$ cells expressing GFP (green) were detected by double immunostaining with antibodies specific for Sox9 and GFP, respectively and nuclei were stained with DAPI (blue). Transverse sections of the thoracic vertebrae at the forelimb level at E10.5 (A-C) and those at the interlimb level on E13.5 (D-F) are shown. Frontal sections of the forelimb at E10.5 (G-I) and sagittal sections of the forelimb at E13.5 (J,K) are also shown. Sagittal sections of the nasal region (L), vertebral column (M), the knee joint (N), and the heel (O) at E14.5 are shown. An arrow in (A-F) indicates the notochord. (C,F,I,J-O) Merged images are presented. Arrowheads in (C) indicate the dorsolateral sclerotome expressing both Sox9 and Scx. An arrowhead and an asterisk in (F) indicate a Scx$^+$ tendon and a Sox9$^+$ rib, respectively. The dotted line in (D), (E), and (F) indicate dorsal root ganglion (drg). Arrowheads in (I) indicate a Scx$^+$/Sox9$^+$ region at the proximal part of the forelimb. Arrowheads in (J) and asterisks in (K) indicate Scx$^+$/Sox9$^+$ regions in the prospective joints of the forelimb. Arrowheads in (M) indicate Scx$^+$ intervertebral regions visualized by GFP expression. An arrow in (N) indicates the developing cruciate ligaments. Femur, tibia, and patella are enclosed by the dotted line. At, Achilles tendon; ca, calcaneus; drg, dorsal root ganglion; fe, femur; me, metacarpal; nc, notochord; ns, nasal septum; nt, neural tube; pa, patella; ph, phalanx; ra, radius; ri, rib; ti, tibia; ul, ulna; vb, vertebral body. Scale bars: 50 μm (K); 100 μm (O); 200 μm (A-C,G-I,L-N); 280 μm (D-F); and 300 μm (J).

Fig. 2. Contribution of *Sox9*$^{+}$ progenitors to the axial tendon and ligament formation.

(**A-E**) Transverse or sagittal sections were prepared from *Sox9*$^{Cre/+}$*;Ai14;ScxGFP* embryos. Cells with the *Sox9*$^{+}$ cell lineage were detected by tdTomato reporter expression. Scx^{+} cells were detected with anti-GFP antibody. (A) A transverse section of the trunk at the thoracic level. Arrowheads indicate the axial tendons associating with vertebrae and ribs. (B) A sagittal section of the vertebral column. The developing intervertebral discs are enclosed by the dotted line. Arrowheads, arrows, and asterisks indicate the intervertebral annulus fibrosus, anterior longitudinal ligament, and nucleus pulposus, respectively. (C) The diaphragm is shown. Arrows in (D) indicate the abdominal tendon in the body wall. (E) The sagittal section of tail is shown. Arrows and arrowheads indicate tendons associated and not associated with the vertebrae in the developing tail, respectively. Rostral and caudal sides are indicated by r and c, respectively. (**F-H**) Frozen frontal sections of the vertebral columns were prepared from *Sox9*$^{Cre/+}$*;Ai14* newborns. Sections at the vertebral bodies (F), the articular process (G), and the spinous process (H) are shown. *Sox9*$^{+}$ cells were detected through the expression pattern of tdTomato (red). Tnmd was visualized by immunostaining with specific antibodies (green). Arrows in (F-H) and arrowheads in (G) and (H) indicate tendons and ligaments associated with the lumbar vertebral column, respectively. ap, articular process; dp, diaphragm; ht, heart; lu, lung; na, neural arch; nt, neural tube; ri, rib; sp, spinous process; st, sternum; vb, vertebral body. Scale bars: 200 μm.

Fig. 3. Contribution of the *Scx*$^{+}$*/Sox9*$^{+}$ cell lineage to the formation of appendicular tendons around the developing entheses and ligaments.

(**A-D**) Distribution of *Scx*-expressing tendons and ligaments (GFP, green) with a *Sox9* expression history (tdTomato, red) were analyzed in a *Sox9*$^{Cre/+}$*;Ai14;ScxGFP* mouse embryo at E14.5. Arrows and arrowheads indicate tendon and ligaments, respectively. (A) A lateral view of the hindlimb is presented. (B-D) Sagittal sections of the hindlimb are shown. The developing digit with the prospective digital joints is shown in (B). White and yellow arrows in (C) indicate the force-transmitting and the anchoring tendons at the lower leg, respectively. The boxed region in (C) is shown at a higher magnification in (D). (**E-I**) Sagittal sections of the knee joint prepared from a *Sox9*$^{Cre/+}$*;Ai14;ScxGFP* embryos at E14.5 (E-G) or a *Sox9*$^{Cre/+}$*;Ai14* newborn mice (H,I) are shown. Developing cartilaginous primordia of the femur and tibia are enclosed by the dotted line. Scx^{+} cells (E,G, green) and Sox9^{+} cells (I, green) were detected by immunostaining with GFP and Sox9 antibodies, respectively. Cells derived from *Sox9*$^{+}$ progenitors were detected via the expression of tdTomato (F,G,H, red). Arrowheads in (H) and (I) indicate ligaments of the knee joint. ca, calcaneus; d4, digit 4; d5, digit 5; fe, femur; fi, fibula; me, metacarpal; ph, phalanx; ti, tibia. Scale bars: 200 μm.

Fig. 4. Distribution of tenocytes derived from the *Sox9*$^{+}$ cell lineage in the forearm and digits.

(**A-L**) Transverse sections of the forearm prepared from a *Sox9*$^{Cre/+}$*;R26R* neonates

are shown. Tnmd^{+} (green) and Chm1^{+} (red) regions were visualized by double-immunostaining (A-F). Descendants of *Sox9^{+}* progenitors were visualized by X-gal staining (G-L). Black or white arrowheads in (A-L) indicate tendons of the forearm. A yellow arrowhead in (B), (H), (F), and (L) indicates ligaments of the forearm. The boxed regions in (E) and (K) are shown at a higher magnification in (F) and (L), respectively. The region enclosed by a white and a black line in (D) and (J) indicates the carpals. The region enclosed by a red dotted line in (C), (D), (I), and (J) indicates the tendons T21 and T22 as defined in Table S1. The region enclosed by a white or a black dotted line in (B-D) and (H-J) indicates tendons T19 and T25 as defined in Table S1. (**M**) Schematic illustration of the distribution of tenocytes or ligamentocytes with a *Sox9^{+}* lineage on the dorsal side of the mouse forearm. Bones (white), muscles (pink), and extensor tendons (light green) are shown. The dark blue color indicates tenocytes and ligamentocytes with a *Sox9^{+}* lineage. ca, carpal bones; hu, humerus; me, metacarpal; ra, radius; ul, ulna. Scale bars: 200 μm.

Fig. 5. Contribution of *Sox9^{+}* progenitors to enthesis formation.

(**A-I**) Sagittal frozen sections of the patella (A-C), the knee joint (D-F), the heel joint (G-I), were prepared from *Sox9$^{Cre/+}$;R26R* newborn mice. Col1^{+} (green in A,D,G), Tnmd^{+} (green in B,E,H), and Chm1^{+} (red in A,B,D,E,G,H) regions were visualized by double-immunostaining. The distribution of X-gal-positive cells with a *Sox9^{+}* lineage in the patella (C), the knee joint (F), and the heel joint (I) is also shown. Arrowheads in (D-F) indicate ligaments in the knee joint. Arrowheads and arrows in (G-J) indicate the Achilles tendon (T9) and the superficial digital flexor tendon (T10), respectively. Yellow

arrows in (B), (E), and (H) indicate the Tnmd/Chm1 double-negative region at the developing enthesis of the cruciate ligaments (L5 and L6 in E), the Achilles tendon (T9 in H) and the patella ligament (L4 in B), respectively. Abbreviations: ca, calcaneus; fe, femur; pa, patella; ti, tibia; tl, talus;. Scal bars: 200 μm.

Fig. 6. Skeletal abnormalities by the loss of *Sox9* in *Scx*$^{+}$/*Sox9*$^{+}$ cells.

(**A,B**) Lateral views of skeletal preparations of control (A), and *ScxCre-L;Sox9*$^{flox/flox}$ embryos (B) at P0. (**C-F**) Dorsal views of the ribcage (C,D) and the vertebral bodies of the lumbar vertebrae (E,F) of control (C,E) and *ScxCre;Sox9*$^{flox/flox}$ at P0 (D,F). Arrows in (E) indicate the transverse process. Asterisks in (E) and (F) indicate intervertebral discs of the lumbar vertebrae. (**G-L**) Appendicular skeletons of control (G,I,K), and *ScxCre-L;Sox9*$^{flox/flox}$ at P0 (H,J,L). Dorsal view of the forelimb (G,H) and lateral view of the hindlimb (I-L) are shown. The elbow joint (G,H), the calcaneous (I,J), and the patella (K) are indicated by an arrow. The dotted line in (K) and (L) encloses the epiphysis of the femur, the tibia, and the patella. (**M-P**) *In situ* hybridization of *Scx* (M,P), *Sox9* (N), and *Myog* (O). Frozen sagittal sections are prepared from wild type embryos at E11.5 (M-O) and E13.5 (P). (M-O) Expression of *Scx* (M), *Sox9* (N), and *Myog* (O) in the costal region at E11.5 is shown. *Scx* is detected in *Sox9*$^{+}$ rib primordia (arrows in M) and in the intercostal region including *Myog*$^{+}$ muscle primordia (O). (P) Expression of *Scx* in the costal region at E13.5 is shown. Arrows in (P) indicate the *Scx*$^{+}$ costal tendons. Ribs are enclosed by the dotted line. cl, clavicle; fe, femur; fi, fibula; hu, humerus; pa, patella; ra, radius; sc, scapula; ti, tibia; ul, ulna; vb, vertebral body. Scale bars: 200 μm.

Fig. 7. Defective formation of the junction between cartilage and tendon/ligament by the loss of *Sox9* in *Scx*$^{+}$/*Sox9*$^{+}$ cells.

(**A-F**) Frontal sections of the sacral (A,B) and the lumbar (C-F) vertebrae of control (A,C,E) and *ScxCre;Sox9*$^{flox/flox}$ at E18.5 (B,D,F). Tnmd^{+} (green) and Chm1^{+} (red) regions were visualized by double-immunostaining (A-D). The transverse processes in control are indicated by arrows in (A) and (C), but those of *ScxCre;Sox9*$^{flox/flox}$ are missing as indicated by arrows in (B) and (D). Asterisks in (A-D) indicate the nucleus pulposus of the intervertebral discs. Sox9^{+} cells are visualized by immunostaining (E,F). Arrows in (E) indicate Sox9^{+} cells in the outer annurus fibrosus of control mice. The dotted line in (E) or (F) encloses the outer annurus fibrosus. (**G,H**) Toluidine blue staining of the sagittal sections of the lumbar vertebrae of control (G) and *ScxCre;Sox9*$^{flox/flox}$ at E18.5 (H). Asterisks in (G) and (H) indicate the nucleus pulposus of the intervertebral disc. Black and gray boxes show width of the inner (in) and the outer (out) annulus fibrosus of the intervertebral disc, respectively. Red bars show width of the vertebral body regions. An arrow indicates intervertebral region. (**I-P**) Sagittal sections of the hindlimb of control (I,K,M,O) and *ScxCre;Sox9*$^{flox/flox}$ E18.5 (J,L,N,P). Tnmd^{+} (green) and Chm1^{+} (red) regions were visualized by double immunostaining (I,K,J,L). Knee joint (I,J) and the attachment site of the Achilles tendon to the calcaneus (K,L) are shown. Arrows in (K) and (L) indicate the junction between hyaline cartilage and the Achilles tendon. Toluidine blue staining (M,N) and Sox9^{+} (red) region visualized by immunostaining (O,P) are shown. The dotted line in (O) or (P) encloses the calcaneus and the Achilles tendon. Arrows in (O) indicate

$Sox9^+$ entheseal cells just adjacent to the hyaline cartilaginous calcaneus. Acl, anterior cruciate ligament; At, Achilles tendon; ca, calcaneus; fe, femur; in, inner annulus fibrosus; out, outer annulus fibrosus; pa, patella; pcl, posterior cruciate ligament; pl, patella ligament; qft, quadriceps femoris tendon; vb, vertebral body; ti, tibia; sdf, superficial digital flexor tendon. Scal Bars: 100 μm (G,H,M-P), 200 μm (A-F,I-L).

Fig. 8. Establishment of the junction between cartilage and tendon/ligament along the *Scx/Sox9* axis.

(**A**) Schematic representation depicting differentiation of the tendogenic, ligamentogenic, and chondrogenic cell lineages along the *Scx/Sox9* axis. The differentiation pathways of $Scx^-/Sox9^+$ chondroprogenitors (CP), $Scx^+/Sox9^+$ teno-/ligamento-/chondro-progenitors (TLCP), and $Scx^+/Sox9^-$ tenoprogenitors (TP) are shown. (**B**) Schematic illustration of the establishment of the chondro-tendinous/ligamentous junction (CTJ/CLJ) to form the osteo-tendinous/ligamentous junction (OTJ/OLJ). $Scx^+/Sox9^+$ progenitors give rise to the primordial CTJ/CLJ. The established CTJ/CLJ further develops to form the OTJ/OLJ during postnatal growth. *Sox9* and *Scx* expression levels are shown by the dark gray-colored and light gray-colored regions, respectively.

Fig. S1. Predominant distribution of $Scx^+/Sox9^+$ cells around the primordial enthesis, the transitional zone from tendon/ligament to cartilage.

(**A-G**) *In situ* hybridization of *Scx* (A,D,E,G), *Sox9* (B,F), and *Myog* (C). Frozen sagittal

sections are prepared from wild type embryos at E13.5 (A-F) and E16.5 (G). Expression of *Scx*, *Sox9*, or *Myog* in the forelimb (A-D) and hindlimb (E-G). An arrowhead in (A) indicates the expression of *Scx* at the myotendinous junction. Arrows in (A) and (B) indicate the insertion sites of tendons of triceps brachii muscles into the olecranon. Humerus and ulna are enclosed by the dotted line (C). Arrows in (D) indicate the *Scx*$^{+}$ ligaments of the digit. Arrows in (E) and (F) indicate the *Scx*$^{+}$/*Sox9*$^{+}$ epiphyseal regions. (G) Expression of *Scx* in the knee joint at E16.5 is shown. Femur, tibia, and patella are enclosed by the dotted line. An arrow in (G) indicates cruciate ligament. ca, calcaneus; fe, femur; fi, fibula; hu, humerus; pa, patella; pl, patella ligament; qtf, quadriceps femoris tendon; ti, tibia; ul, ulna. Scale bars: 200 μm.

Fig. S2. Distribution of Sox9^{+} and Sox9^{-} cells in the Scx^{+} region of ScxGFP mouse embryo at E11.5.

(**A-F**) In *ScxGFP* transgenic mouse embryos, Sox9^{+} (red) and Scx^{+} cells that are labeled by GFP (green) were detected by double immunostaining with antibodies specific for Sox9 and GFP, respectively; nuclei were stained with DAPI (blue). Merged images are presented in (C) and (F). Transverse section of a thoracic level (A-C) and forelimb (D-F) of *ScxGFP* mouse are shown. Arrows in (A)-(C) indicate notochord. Arrowheads in (C) and (F) indicate Scx^{+}/Sox9^{+} region in the proximal rib (C) and proximal forelimb (F), respectively. The dotted line in (A) and (B) indicate dorsal root ganglions. drg, dorsal root ganglion; nc, notochord; nt, neural tube; ri, rib. Scale bars: 200 μm.

Fig. 1

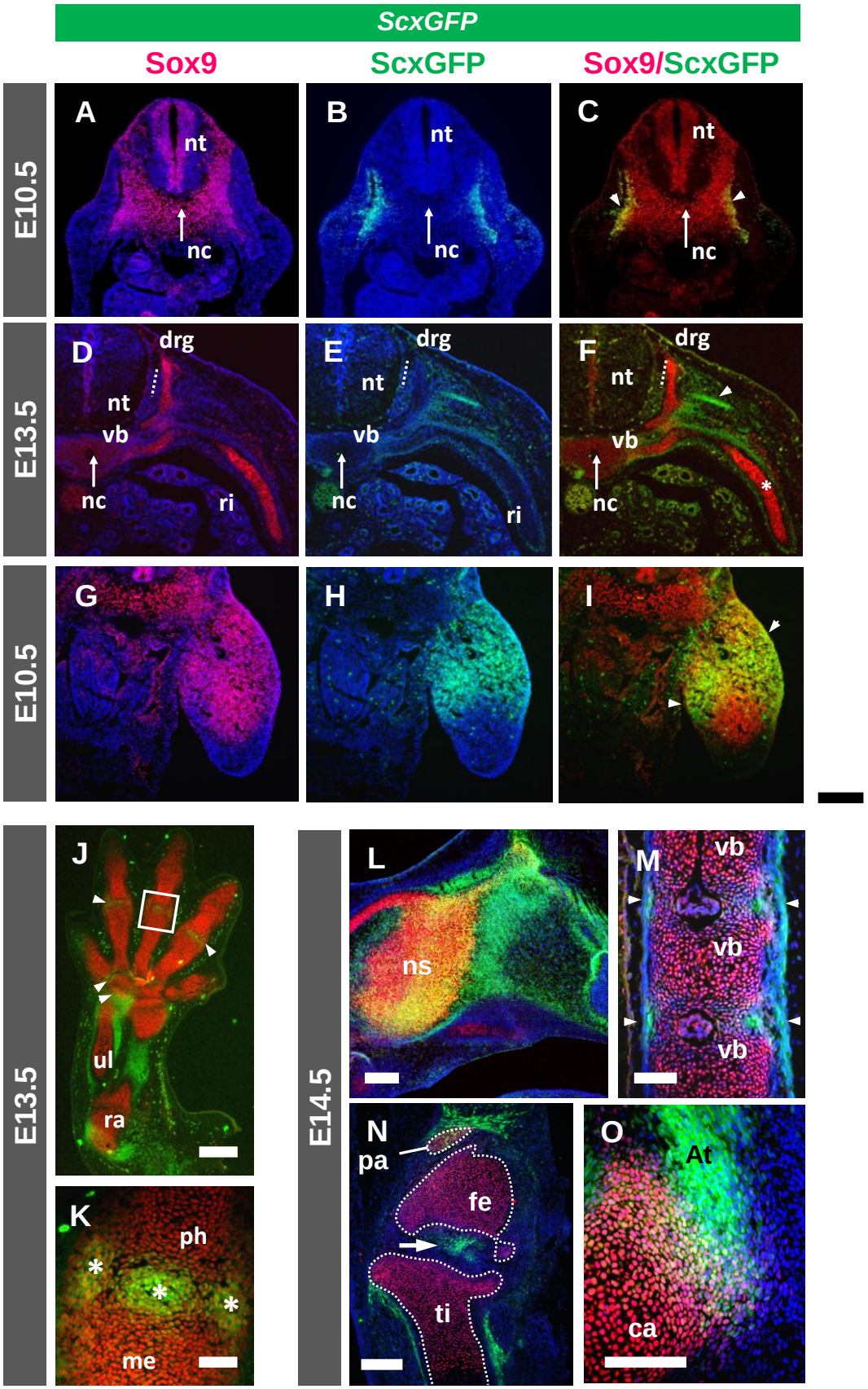
ScxGFP
Sox9
ScxGFP
Sox9/ScxGFP
E10.5
E13.5
E10.5
E13.5
E14.5
A
B
C
D
E
F
G
H
I
J
K
L
M
N
O
nt
nc
drg
vb
ri
ul
ra
ph
me
ns
pa
fe
ti
At
ca

Fig. 2

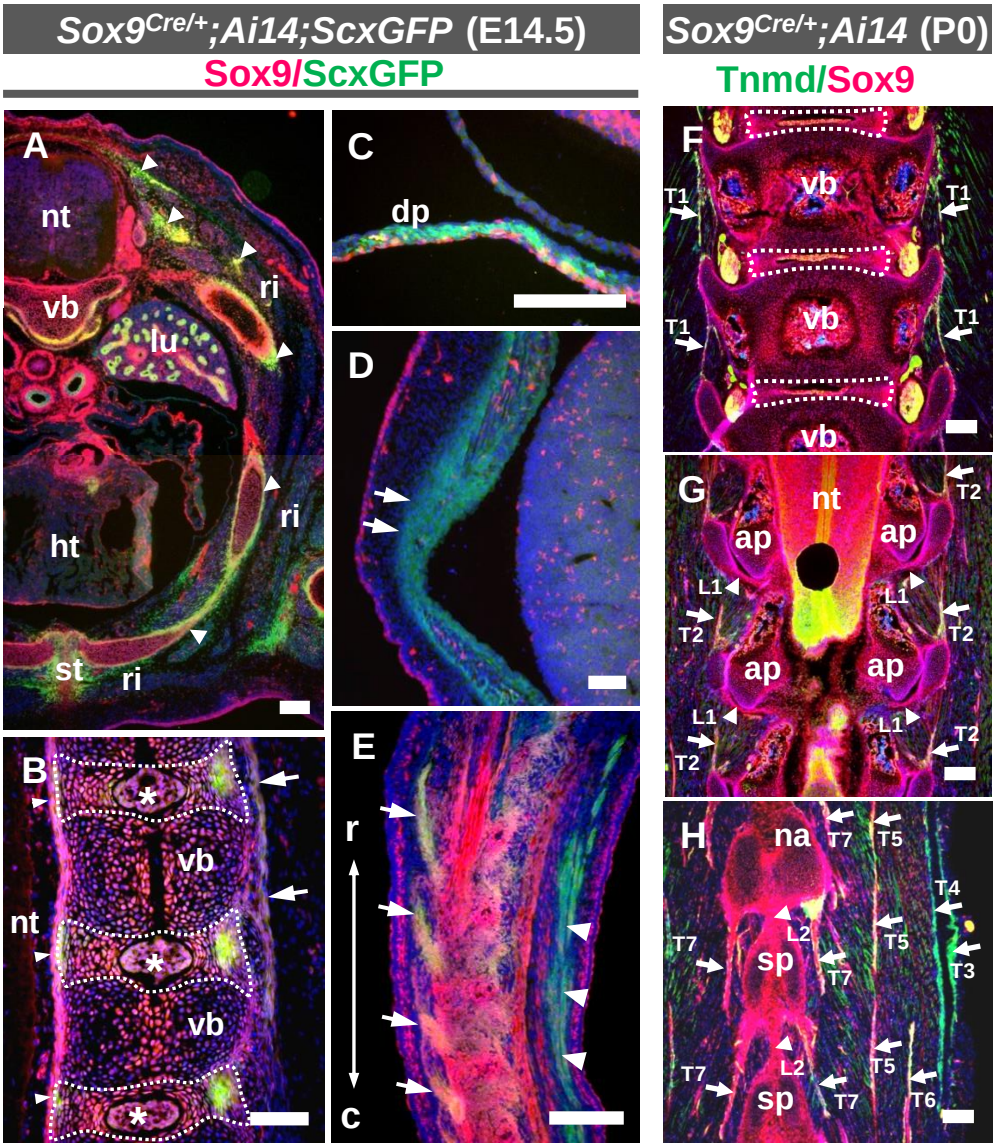
Sox9Cre/+;Ai14;ScxGFP (E14.5)
Sox9/ScxGFP
Sox9Cre/+;Ai14 (P0)
Tnmd/Sox9
A
nt
ri
vb
lu
ri
ht
st
ri
C
dp
D
B
vb
nt
vb
E
r
c
F
T1
vb
T1
T1
vb
T1
vb
G
nt
T2
ap
ap
L1
L1
T2
T2
ap
ap
L1
L1
T2
T2
H
na
T7
T5
T4
T7
L2
T5
T3
sp
T7
T7
L2
T5
sp
T7
T6

Fig. 3

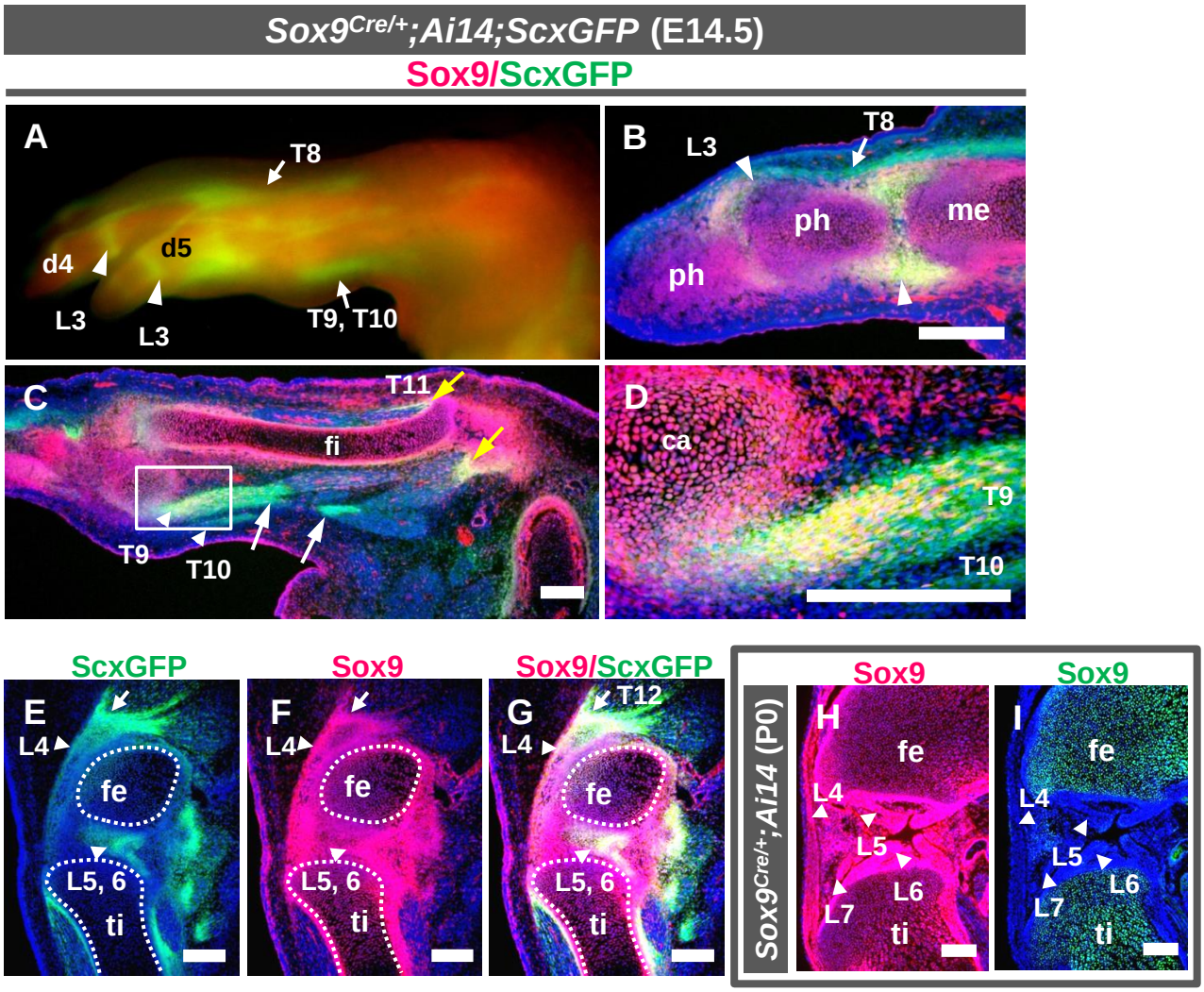
Sox9Cre/+;Ai14;ScxGFP (E14.5)
Sox9/ScxGFP
A
T8
d4
d5
L3
L3
T9, T10
B
L3
T8
ph
me
ph
C
T11
fi
T9
T10
D
ca
T9
T10
ScxGFP
Sox9
Sox9/ScxGFP
E
L4
fe
L5, 6
ti
F
L4
fe
L5, 6
ti
G
T12
L4
fe
L5, 6
ti
Sox9Cre/+;Ai14 (P0)
Sox9
Sox9
H
fe
L4
L5
L6
L7
ti
I
fe
L4
L5
L6
L7
ti

Fig. 4

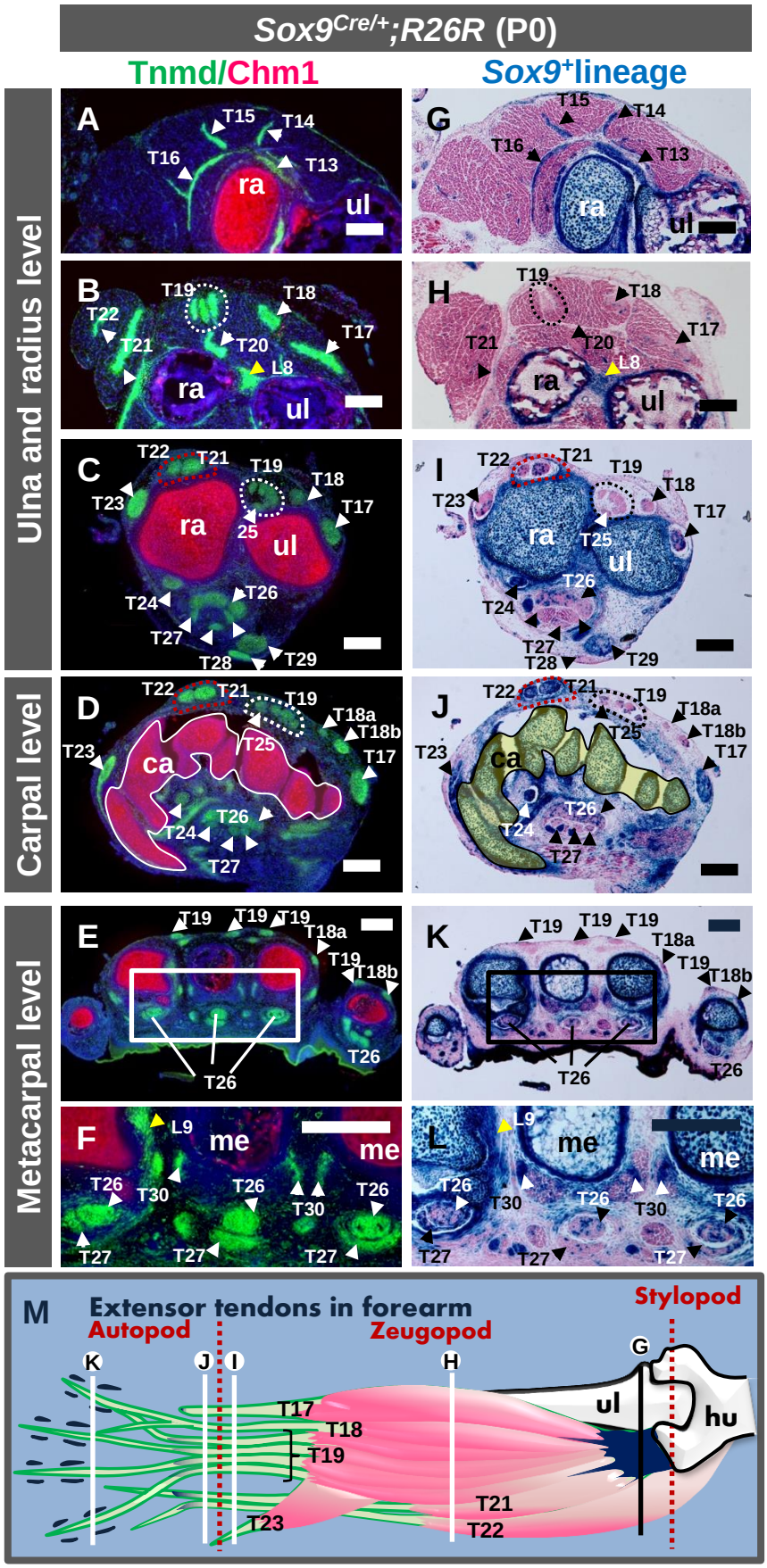
Sox9Cre/+;R26R (P0)
Tnmd/Chm1
Sox9+lineage
Ulna and radius level
Carpal level
Metacarpal level
A
B
C
D
E
F
G
H
I
J
K
L
M
Extensor tendons in forearm
Autopod
Zeugopod
Stylopod
ra
ul
ca
me
hu
T15
T14
T16
T13
T19
T18
T22
T21
T20
T17
L8
T23
25
T24
T26
T27
T28
T29
T18a
T18b
T25
L9
T30

Fig. 5

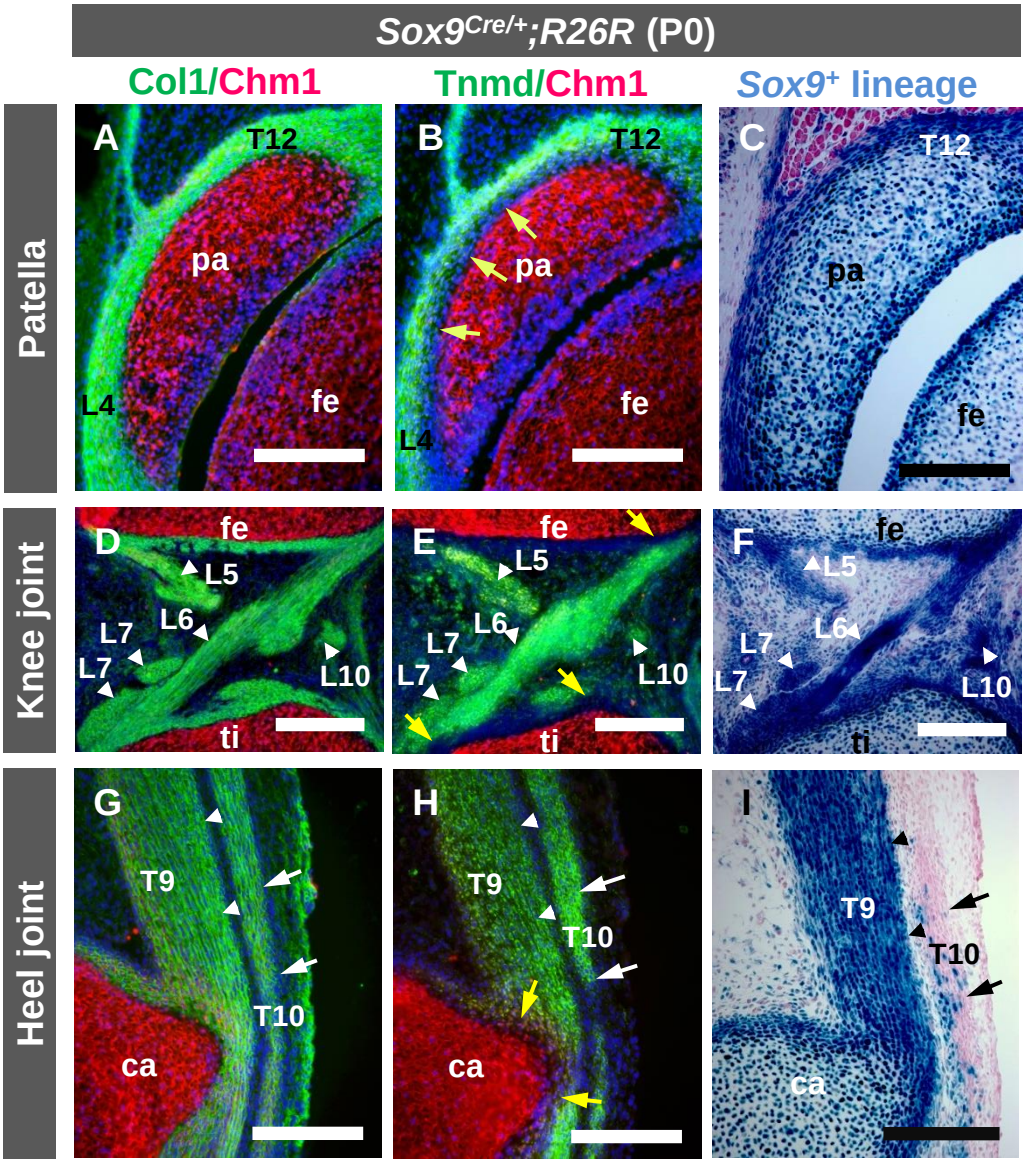
Sox9Cre/+;R26R (P0)
Col1/Chm1
Tnmd/Chm1
Sox9+ lineage
Patella
Knee joint
Heel joint
A
B
C
D
E
F
G
H
I
T12
pa
fe
L4
L5
L6
L7
L10
ti
T9
T10
ca

Fig. 6

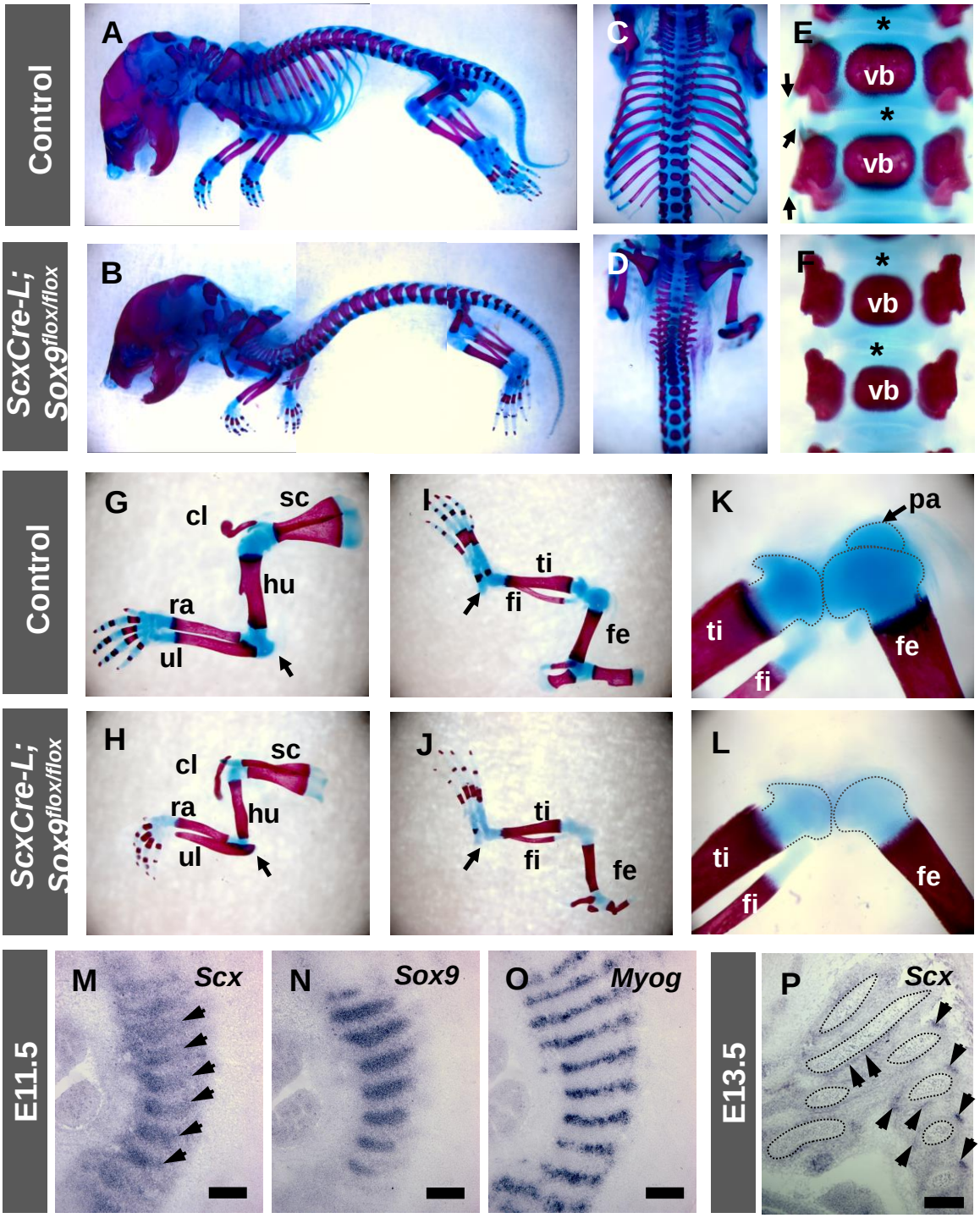
Control
ScxCre-L; Sox9flox/flox
A
B
C
D
E
F
vb
vb
vb
vb
Control
ScxCre-L; Sox9flox/flox
G
H
I
J
K
L
cl
sc
hu
ra
ul
ti
fi
fe
pa
E11.5
E13.5
M
N
O
P
Scx
Sox9
Myog
Scx

Fig. 7

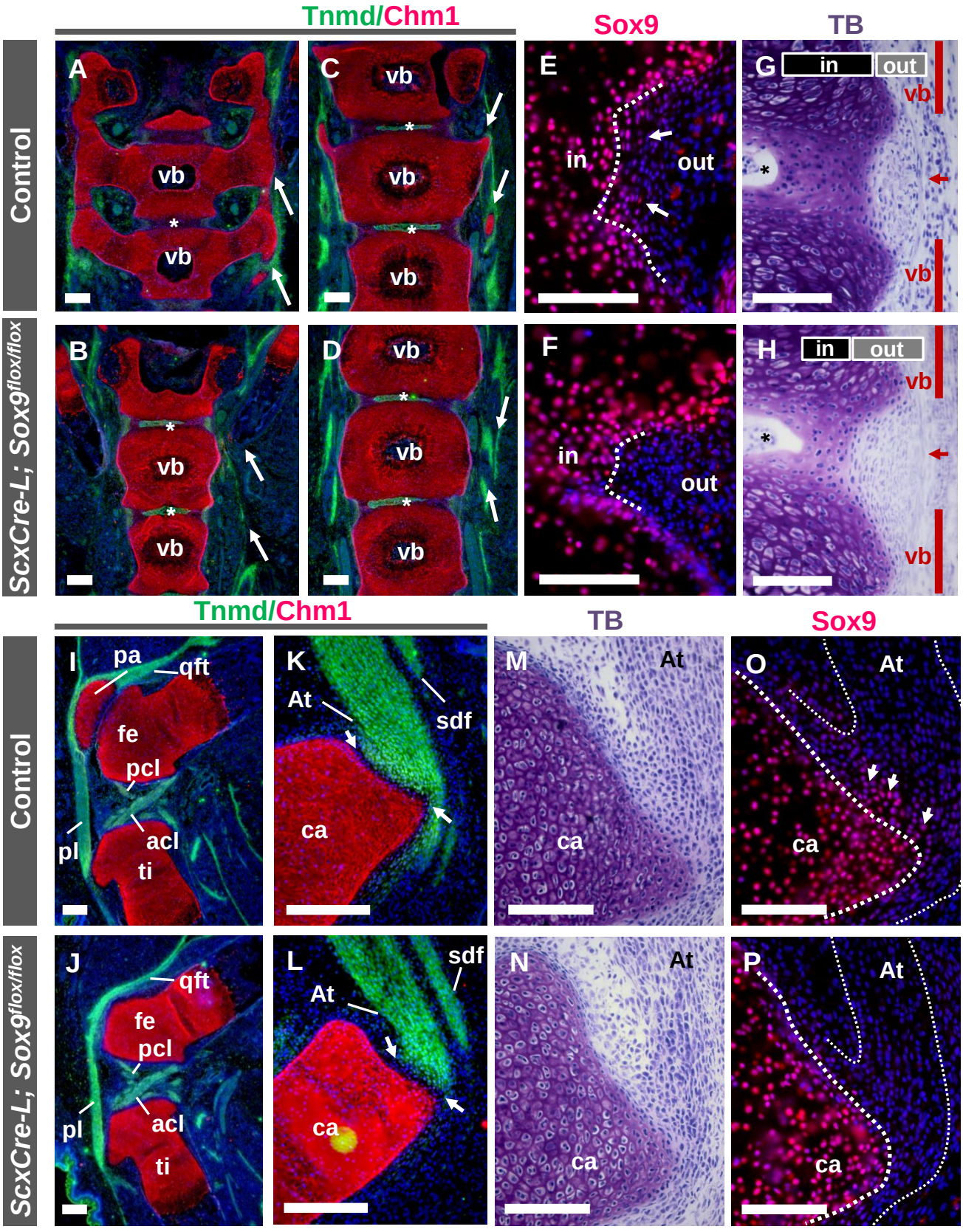
Tnmd/Chm1
Sox9
TB
Control
ScxCre-L; Sox9flox/flox
A
B
C
D
E
F
G
H
vb
*
in
out
Tnmd/Chm1
TB
Sox9
Control
ScxCre-L; Sox9flox/flox
I
J
K
L
M
N
O
P
pa
qft
fe
pcl
pl
acl
ti
At
sdf
ca

Fig. 8

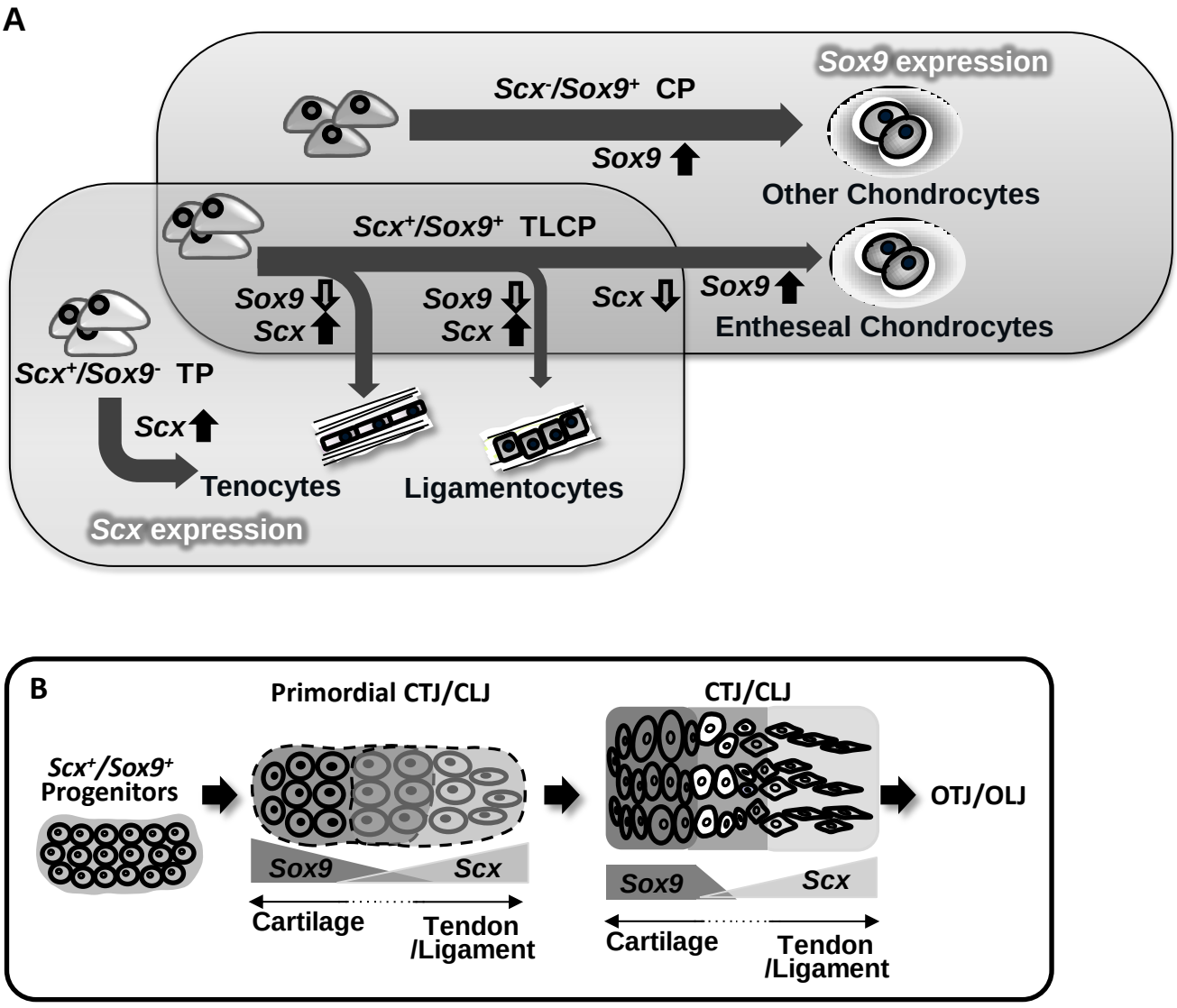
A
Sox9 expression
Scx-/Sox9+ CP
Sox9
Other Chondrocytes
Scx+/Sox9+ TLCP
Sox9
Scx
Sox9
Scx
Scx
Sox9
Entheseal Chondrocytes
Scx+/Sox9- TP
Scx
Tenocytes
Ligamentocytes
Scx expression
B
Primordial CTJ/CLJ
CTJ/CLJ
Scx+/Sox9+
Progenitors
OTJ/OLJ
Sox9
Scx
Sox9
Scx
Cartilage
Tendon
/Ligament
Cartilage
Tendon
/Ligament

Supplemental Fig. 1

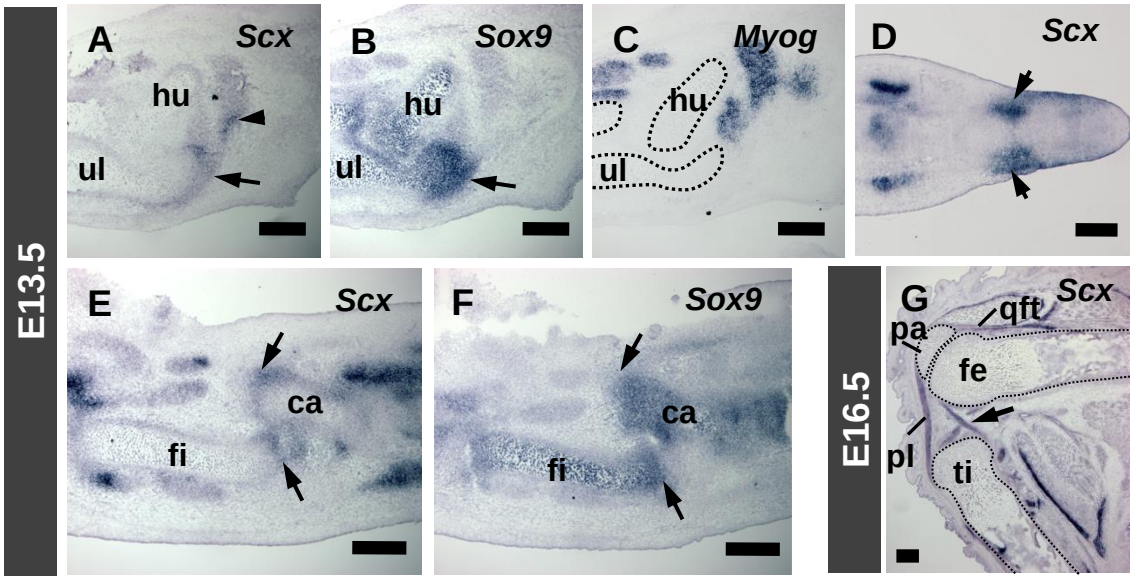

Supplemental Fig. 2

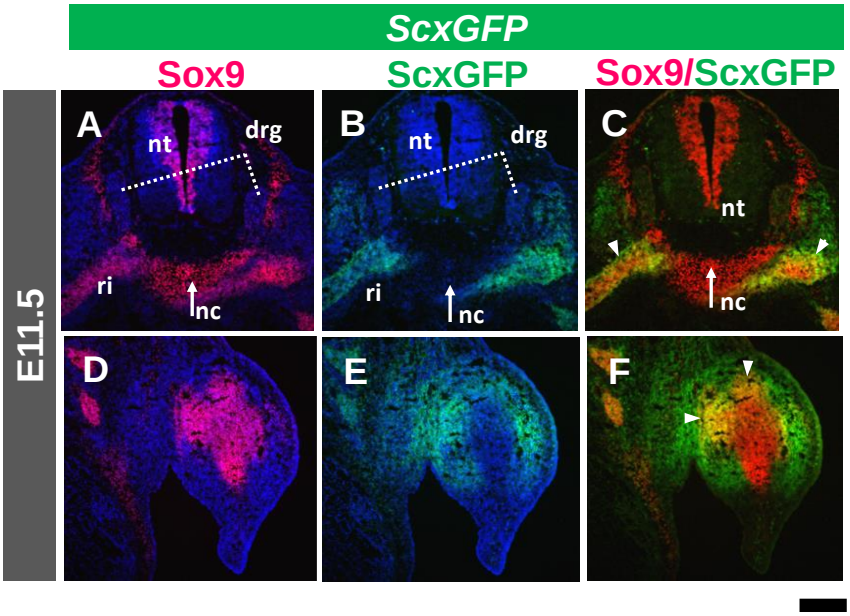

Table S1

Nomenclature of tendons in this study

No.[a]	A/F[b]	Nomenclature of tendons
T1		Thoracolumbar fascia (anterior layer)
T2	A	Origin of longissimus muscle
T3	A	Origin of latissimus dorsi muscle
T4		Thoracolumbar fascia
T5	A	Origin of longissimus muscle
T6	A	Origin of iliocostalis lumborum muscle
T7	A	Origin of multifidi muscle
T8	F	Extensor digitorum longus tendon
T9	F	Achilles tendon
T10	F	Superficial digital flexor tendon
T11	A	Origin of tibialis anterior muscle
T12	F	Quadriceps femoris tendon
T13	A	Origin of pronator muscle
T14	A	Common extensor tendon
T15	A	Common extensor tendon
T16	A	Origin of pronator muscle
T17	F	Extensor carpi ulnaris tendon
T18	F	(a) Extensor digiti quarti tendon
	F	(b) Extensor digiti quinti tendon
T19	F	Extensor digitorum communis tendon
T20	A	Origin of extensor pollicis muscle
T21	F	Extensor carpi radialis brevis tendon
T22	F	Extensor carpi radialis longus tendon
T23	F	Extensor pollicis tendon
T24	F	Flexor carpi radialis tendon
T25	F	Extensor indicis proprius tendon
T26	F	Flexor digitorium profundus tendon
T27	F	Flexor digitorium sublimis tendon
T28	F	Palmaris longus tendon
T29	F	Flexor carpi ulnaris tendon
T30	F	Interosseous

Nomenclature of ligaments in this study

No.[c]	Nomenclature of Ligaments
L1	Facet joint capsule
L2	Interspinal ligament phalangeal
L3	Collateral ligament of phalangeal joint
L4	Patella ligament
L5	Posterior cruciate ligament
L6	Anterior cruciate ligament
L7	Transverse ligament of knee
L8	Antebrachial interosseus membrane
L9	Collateral ligament of metacarpophalangeal joint

[a]T1-T30 indicate tendons in this study.
[b]A/F indicates anchoring or force-transmitting tendons.
[c]L1-L9 indicate ligaments in this study.